



A Novel SPN based Multiple RGB Images Security over the Residue Classes of Quaternion Integers $H[K]_\delta$

Muhammad Sajjad^{1,*}, Nawaf A. Alqwaify^{2,*}

¹ NUTECH School of Applied Science and Humanities, National University of Technology,
Islamabad, 44000, Pakistan

² Department of Electrical Engineering, College of Engineering, Qassim University,
Saudi Arabia

Abstract. In this paper, we propose a Substitution and Permutation Network (SPN)-based encryption scheme for secure multiple RGB images over the residue classes of quaternion integers $H[K]_\delta$. In this context, the new construction of $n \times n$ substitution boxes (S-boxes) using quaternion integers is proposed in order to enhance cryptographic strength. The traditional approaches for S-boxes are mostly based on Gaussian, Eisenstein, and elliptic curves, but quaternion integers are a four-dimensional algebra that is somewhat different mathematically, and these provide additional resistance in terms of cryptographic attacks. The strong security attributes of the designed S-boxes. As for multiple RGB image encryption, in order to achieve both confusion and diffusion, the proposed method employs the SPN framework and quaternion integer-based S-boxes. Structured SPN framework based on substitution, permutation, and XOR operations used by the encryption algorithm. It is shown that the encryption method proposed greatly increases the resistance against statistical, differential, and cryptanalytic attacks. The quaternion integer-based encryption framework is used to convey the confidentiality and integrity of multiple RGB images, which promises to be a good solution for secure multimedia applications. The results confirm that quaternion integer algebra can constitute a useful basis for constructing resilient cryptographic primitives for the modern digital security challenges.

2020 Mathematics Subject Classifications: 16S38, 11T71, 94A60

Key Words and Phrases: Quaternion integers, Multiple RGB Image Encryption, SPN, Confusion, Diffusion, Security Analysis

1. Introduction

To safeguard multimedia content from unauthorized access, tampering, and cyber threats, advanced cryptographic techniques have emerged in response to the evolving landscape of digital communication and data sharing. Traditionally these include AES

*Corresponding author.

*Corresponding author.

DOI: <https://doi.org/10.29020/nybg.ejpam.v18i2.6228>

Email addresses: muhammad.sajjad@nutech.edu.pk (M. Sajjad), nkoiefly@qu.edu.sa (N. A. Alqwaify)

18 and RSA-type schemes but have been rendered less viable due to challenges like the quan-
19 tum computing threat and so on; thus, we now have more resilient approaches like post-
20 quantum cryptography (PQC), homomorphic encryption and lattice-based cryptosystems.
21 Although encryption in multimedia security is not sufficient, further mechanisms such as
22 digital watermarking, steganography, and perceptual hashing are incorporated for authen-
23 ticity and copyright protection while allowing for secure content distribution. In addition,
24 chaos-based encryption methods and cryptographic models built using deep learning have
25 established a place for them, as they allow for improvement over randomness and adapt-
26 ability, thus making them ideally suitable to face off against statistical and differential
27 attacks. Since the development of blockchain technology, secure multimedia transactions
28 have also been explored on the basis of security frameworks that are decentralized the
29 need, on the one hand, to depend on centralized authorities and, on the other hand, to
30 guarantee traceability and integrity in these transactions. Cryptography also becomes
31 more optimized for reducing stronger security mechanisms through artificial intelligence
32 and machine learning by increasing synergy with cryptography [1]. This means that adap-
33 tive security can be done that focuses on real-time threats in multimedia communications.

34

35 The primary component of non-linearity in block ciphers is substitution boxes (S-
36 boxes), which are very important components to strengthen the crypto security because
37 they provide confusion and are immune to cryptanalytic attacks. This design of an optimal
38 S-box balances various cryptographic properties such as high nonlinearity, low differential
39 uniformity, and minimum probability of linear approximation to make the S-box robust
40 against linear and differential cryptanalysis. Current S-box construction approaches are
41 based on algebraic structures, specifically in the form of finite fields; however, there have
42 been a number of developments in constructing S-boxes from a more sophisticated al-
43gebraic domain, i.e., Gaussian and Eisenstein integers, quaternion algebras, and Galois
44 fields, to increase their cryptographic strength. Furthermore, S-boxes are generated dy-
45namically by evolutionary algorithms, artificial intelligence techniques and deep learning
46 models according to the needs of an evolving security challenge. Currently, modern encryp-
47tion protocols start introducing dynamic and key-dependent S-boxes in order to introduce
48additional complexity and make the cryptographic systems less vulnerable with respect to
49the adaptive attacks. However, their application is not limited to the conventional ciphers
50but also extends to the transparent braiding ciphers, where they are found important in
51the areas of lightweight cryptography, chaotic encryption schemes, and secure image pro-
52cessing, where the nonlinearity in them is a very effective means of providing security of
53data and unpredictability of data [2, 3].

54

55 The single and multiple image RGB encryption is a very complex task which must be
56 done to ensure confidentiality, integrity, and resistance to tax attacks while retaining the
57 visual data quality. In contrast to grayscale images whose pixel intensity values lie in only
58 one channel, RGB images contain three interdependent color channels, and consequently
59 there exist specialized encryption techniques to deal with the multi-dimensional structure
60 of the RGB images. Pixel-level permutation and diffusion mechanisms are conventional;

61 modern approaches involve the use of chaos theory, fractal geometry or DNA encryption
62 with strength of security and efficiency. Furthermore, the encryption over quaternion and
63 Eisenstein integer domains is also more robust by bringing in structurally higher dimen-
64 sions into the algebraic structures, thereby enhancing randomness and intrinsic security.
65 For multiple image encryption applications, joint encryption schemes, compressive sens-
66 ing, etc., are used for simultaneous encryption and, at the same time, keeping complexity
67 low. Moreover, real-time image encryption using a hybrid model that improves adapt-
68 ability and efficiency was also explored by combining deep learning and cryptographic
69 techniques. Moreover, robust encryption mechanisms for RGB multimedia data are de-
70 sired due to the increasing demand for secure image transmission in medical imaging,
71 surveillance, etc [4, 5].

72

73 Quaternion integers allow us to move past complex numbers and take an extension of
74 algebra into a four-dimensional algebraic system with some unique properties that have
75 been used in cryptography, coding theory and secure communications. Quaternion alge-
76 bras are defined as the non-commutative extension of the Gaussian and Eisenstein integers
77 and yield a rich mathematical framework in which one can define cryptographic primitives
78 with enhanced security characteristics. Such inherent structure allows the development of
79 SPNs with improved confusion and diffusion properties and secure realization of encryp-
80 tion schemes. Quaternion-based constructions in error-correcting codes help in robust
81 channel coding techniques, which enhance the data reliability in a noisy communication
82 environment. Moreover, quaternion integer-based cryptosystems have also been used for
83 public key encryption, digital signatures and secure key exchange protocols using their
84 algebraic complexity that makes them resistant to conventional cryptanalytic attacks. In-
85 deed, recent research also explores their usage in image and signal processing, specifically
86 in extracting new and secure features in image and signal representation. Also, with the
87 growing evolution in the security threats, the integration of quaternion-based mathemat-
88 ical structures in the modern cryptographic systems can open a way to develop enhanced
89 configurable cryptographic information spread algorithms with high performance and en-
90 hanced resistance towards the modern attack vectors [6–8].

91

92 To begin with, the encryption system is based on algebraic structures and multimedia
93 security, which is now a key component in the encryption schemes. On the other hand,
94 Menezes et al. [1] report in detail traditional cryptographic methods which offer strong and
95 secure communications. These challenges, however, call for the adoption of the advanced
96 mathematical structures with quaternion integers, which allow more algebraic properties
97 in the encryption and error correction [6]. Ozen and Guzeltepe [9, 10], which bring the
98 use of quaternion integers into cyclic codes, and hence into robust encryption schemes.
99 Shah and Rasool [8] also develop this research by demonstrating how quaternion-based
100 coding can be advantageous in secure data transmission. More recently, Sajjad and Shah
101 [7] suggest a version of the Berlekamp–Massey algorithm for decoding cyclic codes over
102 quaternion integers, which further confirms their cryptographic power. Additionally, Saj-
103 jad et al. [11] give higher-length cyclic codes based on quaternion integers as well as new

104 decoding algorithms for better error resilience. S-boxes are fundamental nonlinear com-
105 ponents in symmetric cryptography to make it secure by introducing confusion. Khan et
106 al. [3] provide more motivation for the construction of strong S-boxes by noting that this
107 remains a focal area of research, and we use chaotic Lorenz systems to construct robust
108 substitution boxes. Carlet and Ding [2] give a comprehensive consideration on how to
109 analyze S-box nonlinearities from a cryptographic point of view. These concepts are then
110 utilized to design S-boxes over Gaussian and Eisenstein integers by Sajjad et al. [12, 13]
111 and shown to be useful in block cipher security. Moreover, in [4] the substitution box
112 generator is introduced that is purpose-built for image encryption together with its exten-
113 sion of quaternion intensity in [14] to achieve enhanced nonlinearity and security. These
114 results have been further optimized in recent research of Artuğer and Özkaynak [15], who
115 applied randomized selection methodologies to S-box nonlinearity.

116
117 In recent years, the increase in multimedia communication has created the need for
118 image encryption, especially with RGB images. An SPN-based RGB image encryption
119 scheme over Gaussian numbers is proposed by Sajjad et al. [5], and it is shown to be more
120 resistant to statistical attacks compared to its counterpart over a finite field. Abd EL-
121 Latif et al. [16] use quantum walk-based pseudorandom number generators for quantum
122 color image encryption, and Ibrahim and Alharbi [17] integrate Henon maps and elliptic
123 curve cryptography to provide efficient image security. Shamsi and Laiphrakpam [18] in a
124 similar fashion widen the scope of multimedia data embedding to the case of audio-based
125 image encryption. Consequently, Wang et al. [19] propose fast encryption based on paral-
126 lel computing, while Cheng et al. [20] use hyperchaotic systems and permutation diffusion
127 architecture to enhance the security. Malik and Shah [21] also design a scheme for multiple
128 image encryption using 3D chaotic maps which utilize the power of chaos theory in mul-
129 timedia security. With the development of many advanced transformations and chaotic
130 systems, the multiple image encryption techniques have become much more complex. Both
131 Yin and Wang [22] use breadth-first search and dynamic diffusion for better randomness,
132 while Wang et al. [23] use DNA sequence operations for chaotic image encryption. Wang
133 et al. [24, 25] recently created hidden attractor chaos systems and conservative hyper-
134 chaotic architectures, which strengthen cryptographic strength even more. Wang and Li
135 [26] also combine Hopfield chaotic neural networks into color image encryption, and Wang
136 and Gao [27] also use Boolean network synchronization. An additional dimension of se-
137 curity is also provided by optical cryptosystems such as asymmetric key cryptosystems
138 for multiple image encryption described by Liu et al. [28]. Xiong et al. [29] is one other
139 well-known contribution based on pixel exchange operations and vector decomposition,
140 and Deng et al. [30] is yet another contribution based on spectral cropping and spatial
141 multiplexing. Li et al. [31] also investigated wang2020imagea wzhou2020novelform-based
142 techniques, which, however, use robust chaotic maps for secure image encryption. Zhang
143 and Wang [32, 33] also extend DNA encoding and 3D permutation models, and Li et al.
144 [31] further improve security using compressive ghost imaging.

145
146 In response to the fast growth of digital communication and multimedia applications,

147 strong security features are required for secure access to sensitive image data from cy-
148 ber or unauthorized access. Traditional methods of encryption using Gaussian integers
149 and Eisenstein integers have been shown to be useful for protecting the content in a dig-
150 ital domain, but the cryptanalysis of such traditional methods has sometimes been too
151 easy [5, 12–14]. It is further evident from the advances in attacks due to increasing so-
152 phistication, including, among others, differential cryptanalysis, linear cryptanalysis, and
153 statistical attacks, that the need for a more resilient cryptographic framework is all the
154 more important [2–4]. Quaternion integers form a non-commutative extension of complex
155 numbers and, as such, furnish more algebraic structure and more security for encryp-
156 tion systems in a higher dimension. Relevant recent research [7, 9–11] has also pointed
157 out quaternion algebra’s possibility to be employed in building cryptographic primitives,
158 in particular, designing S-boxes and encrypting frameworks. Indeed, the employment of
159 quaternion integers in cryptographic applications offers some unique advantages, such as
160 increased diffusion and confusion properties, less algebraic complexity, and a larger key
161 space that aids in combating different attacks [5, 13, 14]. As a result, encryption schemes
162 based on Substitution Permutation Network (SPN) are found to be very effective for secure
163 image encryption. SPN frameworks based on S-boxes over finite fields like $GF(2^n)$, elliptic
164 curves or Gaussian integers, remain vulnerable to cryptanalysis for the reason that they
165 have algebraic properties [12, 13]. This is a novel cryptographic primitive based on quater-
166 nion integer-based S-boxes which augment the nonlinearity and differential uniformity of
167 the encryption process by introducing quaternion integer-based S-boxes into the utilization
168 of the SPN structure [5, 14]. The rationale behind this study is that a very secure multiple
169 RGB image encryption system based on the mathematical strength of quaternion integers
170 is to be developed. The proposed approach is to use quaternion-integer-based S-boxes to
171 integrate the security of digital images against multiple attacks with good efficiency of
172 computation [5, 13, 14]. In terms of multimedia security, this research adds an innovative
173 cryptographic model in the form of combining algebraic developments and pragmatic en-
174 cryptation mechanisms to address the fast-emerging difficulties that digital data protection
175 in modern communication systems faces.

176
177 The goal of this research is to propose a new cryptographic framework, among whose
178 building blocks are quaternion integers, which improve the security of conferences where
179 several RGB images are being displayed at once. Another one of the key contributions
180 is the formation of an original way to create $n \times n$ S-boxes based on quaternion inte-
181 gers. In contrast to other S-box designs based on Gaussian or Eisenstein integers, elliptic
182 curves or chaotic functions, the proposed method is algebraically distinct in that it uses
183 the exceptional four-dimensional algebraic structure of quaternion integers. As for the
184 generated S-boxes, the non-commutative nature of quaternion multiplication allows for
185 much more nonlinear, differential uniform, and strict avalanche characteristics than can
186 be obtained using finite field techniques, which makes it highly resistant to linear and dif-
187 ferential cryptanalysis. Finally, the proposed framework uses these S-boxes as substitution
188 and permutation elements of an SPN, with the aim of guaranteeing a high degree of con-
189 fusion and diffusion properties to achieve secure multimedia encryption. The work makes

190 another considerable contribution by introducing a fast multi-image encryption scheme
 191 which allows processing multiple RGB images simultaneously. The encryption scheme
 192 has been designed with strong security features and efficient computation, ideal for ap-
 193 plication in real time, such as secure cloud storage, medical imaging, video surveillance,
 194 etc. Statistical tests, entropy measurement, correlation analysis and differential attack
 195 resistance are rigorously performed on the proposed method, and it is shown to achieve
 196 superior performance in terms of security when compared with the existing techniques.
 197 In addition, this research points out the ability of quaternion integers to be used in the
 198 analogical cryptographic applications and lays a foundation for future studies of more
 199 high-dimensional algebraic structures, which can be used for encryption. The results lead
 200 us to conclude that the proposed system is practical and efficient, which helps to advance
 201 secure multimedia communication.

2. Quaternion Integers

202
 203 By following [7–11], let $\mathbb{H}(\mathbb{R})$ be the Hamilton quaternion algebra over the real numbers
 204 \mathbb{R} . It is a non-commutative but associative unital algebra if it satisfies the following
 205 conditions.

- 206 • $\mathbb{H}(\mathbb{R}) = \{a_0 + a_1i + a_2j + a_3k : \forall a_i \in \mathbb{R}\}$ is a free \mathbb{R} -module with basis $\{\pm 1, \pm i, \pm j, \pm k\}$.
- 207 • Element 1 is the multiplicative identity.
- 208 • Operations on the basis elements $\pm 1, \pm i, \pm j, \pm k$ are given in Figure. 1.

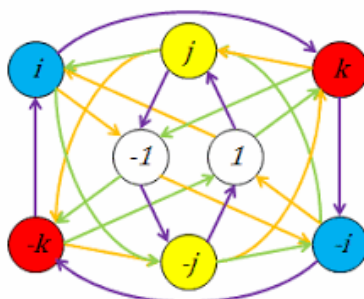


Figure 1: Multiplication of basis elements

209 The ring of quaternion $H(\mathbb{Z}) = \{b_0 + b_1i + b_2j + b_3k : \text{for all } b_0, b_1, b_2, b_3 \in \mathbb{Z}\}$ contained
 210 in $H(\mathbb{R})$, where \mathbb{Z} is the ring of integers. If $q = b_0 + b_1i + b_2j + b_3k$ is a quaternion integer,
 211 then $\bar{q} = b_0 - b_1i - b_2j - b_3k$ is the quaternion conjugate of q . Let $N(q) = q\bar{q} = b_0^2 + b_1^2 + b_2^2 + b_3^2$
 212 be the norm of q . A quaternion integer q has only two parts: one is the scalar part (S.P.)
 213 b_0 and the other is the vector part (V.P.) $b_1i + b_2j + b_3k$. In a quaternion, the commutative
 214 property of multiplication does not hold. It is possible only in the case of two vector parts
 215 of quaternion integers being parallel.

2.1. Subring of the Quaternion Integer Ring [7, 11]

Define $H(K)$ as:

$$H(K) = \{a + bU \mid a, b \in \mathbb{Z}\},$$

where $U = i + j + k$. Hence, $H(K)$ is a subring of the quaternion integer ring $H(\mathbb{Z})$, and also the commutative property of multiplication holds $H(K)$.

2.2. Sum and Product of Two Quaternions [6]

Let $q_1 = c_0 + c_1i + c_2j + c_3k$ and $q_2 = d_0 + d_1i + d_2j + d_3k$ be two quaternion integers. Then, their sum $q_1 + q_2$ and product q_1q_2 will also be quaternion integers as:

$$q_1 + q_2 = (c_0 + c_1i + c_2j + c_3k) + (d_0 + d_1i + d_2j + d_3k)$$

$$= (c_0 + d_0) + (c_1 + d_1)i + (c_2 + d_2)j + (c_3 + d_3)k = e_0 + e_1i + e_2j + e_3k = q_3.$$

$$q_1q_2 = (c_0 + c_1i + c_2j + c_3k)(d_0 + d_1i + d_2j + d_3k)$$

$$= c_0d_0 + c_0d_1i + c_0d_2j + c_0d_3k + c_1d_0i - c_1d_1 + c_1d_2k - c_1d_3j + c_2d_0j - c_2d_1k - c_2d_2 + c_2d_3i + c_3d_0k + c_3d_1j - c_3d_2i - c_3d_3$$

$$= (c_0d_0 - c_1d_1 - c_2d_2 - c_3d_3) + (c_0d_1 + c_1d_0 + c_2d_3 - c_3d_2)i$$

$$+ (c_0d_2 + c_2d_0 + c_3d_1 - c_1d_3)j + (c_0d_3 + c_3d_0 + c_1d_2 - c_2d_1)k$$

$$= g_0 + g_1i + g_2j + g_3k = q_4.$$

Theorem 1. [3, 11], the set of natural numbers for each odd rational prime p , there exists a prime $\delta \in \mathbb{H}(\mathbb{Z})$ such that,

$$N(\delta) = p = \delta\bar{\delta},$$

in particular, p is not prime in $\mathbb{H}(\mathbb{Z})$.

Theorem 2. [3, 11], let $\delta \in \mathbb{H}(\mathbb{Z})$ be prime in $\mathbb{H}(\mathbb{Z})$ if and only if $N(\delta)$ is prime in \mathbb{Z} .

Definition 1. [3, 11], let $\mathbb{H}(K)_\delta$ be the residue class of $\mathbb{H}(K)$ modulo δ , where $\delta = a + bU$. Then the modulo function is defined as:

$$\phi : \mathbb{H}(K) = \{a + bU : a, b \in \mathbb{Z}\} \rightarrow \mathbb{H}(K)_\delta,$$

$$\phi(q) = z \pmod{\delta} = q - \left[\frac{q\bar{\delta}}{p} \right] \delta,$$

where $z \in \mathbb{H}(K)_\delta$, and the brackets $[\cdot]$ denote rounding to the nearest integer. To perform quaternion integer (QI) rounding, the scalar part (S.P.) and the coefficient of the vector part (C.V.P.) must be independently rounded to the nearest integers.

235 **Definition 2.** [3, 11], let $\beta, \rho \in \mathbb{H}(K)_\delta$ and define $\alpha = \beta - \rho = (b_0 + b_1i + b_2j + b_3k)$
 236 mod δ . The quaternion Mannheim weight $W_{QM}(\alpha)$ is defined as:

$$W_{QM}(\alpha) = |b_0| + |b_1| + |b_2| + |b_3|.$$

237 The quaternion Mannheim distance $d_{QM}(\rho, \beta)$ between β and ρ is then given by:

$$d_{QM}(\rho, \beta) = W_{QM}(\alpha).$$

238 **Remark 1.** [11], indeed, quaternion Mannheim weight W_{QM} is metric.

239 **Theorem 3.** [7], if $\gcd(a, b) = 1$, then

$$\mathbb{H}(K)/\langle a + b(i + j + k) \rangle \cong \mathbb{Z}_{a^2+3b^2}.$$

240 **Proposition 1.** [7], let $\delta_k = a_k + b_k(i + j + k)$ be distinct primes in $\mathbb{H}(K)$, and let
 241 $p_k = \mathbb{Z}_{a_k^2+3b_k^2}$ be distinct primes in \mathbb{Z} , for $k = 1, 2, 3, \dots, m$. If g is a generator of $\mathbb{H}(K)_{\delta^k}$,
 242 then

$$g^{\frac{\varphi(p^k)}{2}} \equiv -1 \pmod{\delta^k}.$$

243 **Proposition 2.** [7], let $\delta_1 = a_1 + b_1(i + j + k)$ be a prime in $\mathbb{H}(K)$, and let $p \in \mathbb{Z}_{a_1^2+3b_1^2}$
 244 be a prime in \mathbb{Z} . If $\mathbb{H}(K)_\delta$ is generated by g , then

$$\alpha^{\frac{\varphi(p)}{2}} \equiv -1 \pmod{\delta}.$$

245 **Corollary 1.** [7], let $\delta = a + b(i + j + k)$ be a quaternion prime in $\mathbb{H}(K)$, such that the
 246 norm $N(\delta) = p = a^2 + 3b^2$ is a prime in \mathbb{Z} . If $\mathbb{H}(K)_\delta$ is generated by α , then

$$\alpha^{\varphi(p)} \equiv 1 \pmod{\delta}.$$

247 **Remark 2.** The group generated by $\langle \alpha \rangle$ in the above Corollary is denoted by \mathcal{Q}_R .

248 3. Quaternion Integers based $n \times n$ S-boxes

249 Substitution boxes (S-boxes) are essential components used in modern cryptography,
 250 introducing confusion in encryption algorithms to enhance their security. Traditionally,
 251 S-boxes are constructed using finite fields. However, recent studies reveal the potential
 252 of quaternion integers to design highly nonlinear and cryptographically resilient S-boxes.
 253 Quaternions, which generalize complex numbers into a four-dimensional non-commutative
 254 algebra, provide unique mathematical properties that offer increased resistance to crypt-
 255 analytic attacks. In the proposed method, the S-box is defined as a $k \times k$ matrix of
 256 quaternion integers. The quaternion algebraic structure is then employed to construct
 257 $n \times n$ ($n \leq k$) S-boxes with desirable cryptographic properties such as high nonlinearity
 258 and low differential uniformity. Quaternion integer elements are systematically selected
 259 and integrated into a secure substitution layer with strong security and sound efficiency.
 260 The construction utilizes an optimization algorithm to enhance cryptographic strength.
 261 **S-Box Construction Steps:**

- 262 (i) Based on definitions and theorems in Section II, a quaternion integer-based cyclic
 263 group, denoted as Q_R , is defined. This group is structured to have an order of $p - 1$.
- 264 (ii) The group Q_R is subjected to the following transformation and mapped to another
 265 quaternion group using a transformation function:

$$g(x_i) = \frac{1}{ax_i^{-1} + b},$$

266 where x_i^{-1} is the multiplicative inverse of x_i in Q_R , and a and b are quaternion
 267 integers. The expression $ax_i^{-1} + b$ must be a non-zero part of the quaternion residue
 268 class.

- 269 (iii) The scalar and vector parts of the resulting quaternion elements are separated to
 270 form the output of the mapping function. These components are processed indepen-
 271 dently in the following steps.
- 272 (iv) Apply modular reduction modulo 2^n to each component (scalar and vector), pro-
 273 ducing two separate sets of order 2^n , denoted as Q_{R_1} and Q_{R_2} .
- 274 (v) Another transformation is applied to both sets Q_{R_1} and Q_{R_2} using the function:

$$h(x_i) = (cx_i + d) \pmod{2^n},$$

275 where c and d are constants carefully selected to ensure the cryptographic properties
 276 such as high nonlinearity and low differential uniformity are met.

- 277 (vi) A secure encryption process is then performed to generate a pair of S-boxes, denoted
 278 S_s and S_v , using quaternion operations. These S-boxes serve as the core nonlinear
 279 components in cryptographic systems to resist various attacks.

280 **Significance of Quaternion-Based S-Boxes:** The use of quaternion integers in the
 281 construction of S-boxes provides several advantages that can enhance both the security
 282 and efficiency of the substitution layers in block ciphers. Unlike traditional finite field-
 283 based S-boxes, quaternion-based S-boxes leverage the non-commutative algebraic structure
 284 of quaternions to introduce increased complexity and resilience to attacks. Due to their
 285 four-dimensional nature, quaternions offer a richer mathematical framework, improving
 286 nonlinearity — a critical attribute against differential and linear cryptanalysis. Quater-
 287 nion integer-based S-boxes exhibit a strong avalanche effect, whereby small changes in
 288 input cause substantial changes in output, thereby enhancing security. Furthermore, such
 289 S-boxes demonstrate low differential uniformity, making differential attacks ineffective, and
 290 maintain bijectivity (one-to-one mapping), which is essential for secure substitution. More-
 291 over, these S-boxes are efficient and scalable, making them ideal for modern cryptographic
 292 applications, including lightweight encryption schemes for resource-constrained environ-
 293 ments such as IoT devices and embedded systems. Consequently, quaternion integer-based
 294 S-boxes emerge as robust and promising alternatives to traditional designs, offering en-
 295 hanced protection against emerging cryptographic threats.

296 4. 8×8 S-boxes over Quaternion Integers and Analysis

297 From quaternion algebra transformations, it is possible to construct 8×8 S-boxes with
 298 scalar and vector parts independently processed. Suppose the quaternion prime

$$\delta = 80 + 31i + 31j + 31k,$$

299 with norm

$$N(\delta) = 9283,$$

300 being prime in \mathbb{Z} , and the generator

$$\alpha = 2 + 19i + 19j + 19k.$$

301 Two S-boxes are constructed distinctively as follows:

- 302 (i) **Scalar Parts S-box S_s** : This S-box S_s is designed by running all the steps as
 303 described above on the real (scalar) part of quaternions. It is mapped using the
 304 ‘inverse affine’ transformation, modular arithmetic, and the transformation function
 305 $h(x_i)$ applied to the input values.
- 306 (ii) **Vector Parts S-box S_v** : This is an S-box created for the vector (pure quaternion)
 307 part, based on the transformation of the i, j, k parts of quaternion elements to make
 308 it resistant to differential attacks.

309 By independently designing S_s and S_v , the resulting S-boxes, the vulnerability to crypt-
 310 analysis is reduced in both cryptographic applications, secure image encryption, and block
 311 ciphers. This is achieved by utilizing the multidimensional algebraic properties of quater-
 312 nions. Tables 1 and 2 contain the completed S-box values.

313 4.1. Nonlinearity

314 S-box nonlinearity (NL) represents a fundamental element of cryptographic strength
 315 because S-boxes use quaternion integer parts to generate separate nonlinearity functions
 316 between scalar and vector components. The S-boxes benefit from quaternion algebra to
 317 achieve their increased complexity since this mathematical framework exploits the multidimensional nature of the structure. The scalar S-box performs computations on quaternion element real parts through modular transformations and permutation mappings along with affine operations, thereby establishing high levels of nonlinearity that counter linear approximations. The vector S-box uses modular exponentiation and rotation-based diffusion together with non-affine substitutions as individual transformations for the pure quaternion components to achieve strong resistance to differential cryptanalysis. The evaluation of S-box nonlinearity depends on calculating their Hamming distances from affine functions to ensure maximum unpredictability in output variations from small input variations. The quaternion structure protects system security through the distribution of mathematical operations among multiple parts, which reduces statistical correlations, making it practically

Table 1: S_s over the scalar part of QI

188	79	28	130	44	234	176	146	215	184	114	17	162	1	199	158
57	71	34	12	212	156	62	179	20	169	124	159	66	196	222	175
244	91	206	132	144	250	116	143	123	96	54	140	217	127	76	174
29	186	183	150	235	22	82	3	161	239	31	5	241	218	48	190
232	118	152	247	119	171	77	134	194	107	133	255	83	111	170	195
10	126	185	115	14	21	226	105	84	245	238	75	47	202	219	137
92	197	85	149	100	253	249	33	55	50	49	164	192	246	43	18
240	108	32	172	64	102	167	237	207	122	68	81	90	69	251	145
16	198	252	181	139	89	182	224	168	151	13	153	4	228	67	242
51	216	128	204	208	9	8	201	135	87	103	220	11	229	56	173
88	97	189	113	209	6	41	138	142	36	205	60	15	160	30	40
177	52	211	141	210	225	166	221	65	112	248	125	178	78	165	59
24	98	73	148	203	136	101	35	131	121	45	42	7	58	109	155
191	214	93	104	2	46	213	80	70	117	200	227	61	180	254	147
231	129	243	187	38	154	230	106	72	99	94	120	19	193	25	37
86	157	26	63	74	0	23	39	27	53	223	110	95	233	163	236

impossible to perform linear approximations. These S-boxes achieve strong confusion and diffusion capabilities through independent scalar and vector part processing, which protects against attacks including linear cryptanalysis, differential cryptanalysis and algebraic attacks. The complex encryption system's strength increases through the combination of quaternion integer algebraic characteristics in substitution processes. The distinct nonlinearity features of quaternion-based S-boxes provide an enhanced cryptographic approach for developing block ciphers along with implementing secure image encryption systems and future cryptographic protocol designs [3, 5, 12, 17]. The research for nonlinearity characteristics and relevant literature review appears in the proposed results in Table 3 as well as Table 4.

4.2. Bit Independent Criteria

It is crucial for enhancing resistance against differential and linear cryptanalysis that the S-boxes over quaternion integers are separately constructed according to the Bit Independent Criteria (BIC) nonlinearity of the scalar and vector parts. The more independent the change of each output bit with respect to changes in input is, the more this criterion is satisfied, and there should be no predictable pattern of any bit. By applying modular transformation and affine mappings to the real part of quaternion elements, the scalar S-box is designed such that each output bit is statistically independent. On the other hand, the vector S box processes the pure quaternion components separately using different modular exponentiation and rotation-based transformations to increase the unpredictability of the output bits. We compute the correlation between pairs of output bits and find that changes in one bit do not affect the others in a way that is predictable. In cryptographic applications this bit independence property is critical, since the presence of such

Table 2: S_v over the scalar part of QI

60	207	156	2	172	106	48	18	87	56	242	145	34	129	71	30
185	199	162	140	84	28	190	51	148	41	252	31	194	68	94	47
116	219	78	4	16	122	244	15	251	224	182	12	89	255	204	46
157	58	55	22	107	150	210	131	33	111	159	133	113	90	176	62
104	246	24	119	247	43	205	6	66	235	5	127	211	239	42	67
138	254	57	243	142	149	98	233	212	117	110	203	175	74	91	9
220	69	213	21	228	125	121	161	183	178	177	36	64	118	171	146
112	236	160	44	192	230	39	109	79	250	196	209	218	197	123	17
144	70	124	53	11	217	54	96	40	23	141	25	132	100	195	114
179	88	0	76	80	137	136	73	7	215	231	92	139	101	184	45
216	225	61	241	81	134	169	10	14	164	77	188	143	32	158	168
49	180	83	13	82	97	38	93	193	240	120	253	50	206	37	187
152	226	201	20	75	8	229	163	3	249	173	170	135	186	237	27
63	86	221	232	130	174	85	208	198	245	72	99	189	52	126	19
103	1	115	59	166	26	102	234	200	227	222	248	147	65	153	165
214	29	154	191	202	128	151	167	155	181	95	238	223	105	35	108

Table 3: NL of the S-box functions

S-boxes	g_1	g_2	g_3	g_4	g_5	g_6	g_7	g_8
S_s	108.00	108.00	106.00	108.00	108.00	104.00	106.00	108.00
S_v	108.00	108.00	106.00	108.00	108.00	104.00	106.00	108.00

351 an S-box renders the linear correlations or differential trails attacked useless. Quaternion-
 352 based S-boxes, due to independent scalar and vector processes of the scalar and vector
 353 parts, spread bit changes over several dimensions, and their complexity and security are
 354 further increased. Because quaternions are inherently multidimensional, the BIC of the
 355 patterns remains very dispersed among bits, rendering algebraic and statistical attacks in-
 356 effective. The properties are such that quaternion-based S-boxes are indeed highly suited
 357 for cryptographic applications like secure encryption, block cipher design, and advanced
 358 data protection mechanisms [12, 13, 17]. Part of the proposed research of BIC is shown
 359 in Tables 5, 6, and 7, which present the results and comparative analysis of the results

Table 4: NL of the S-box functions

S-boxes	Schemes	Nonlinearity
S_s	Proposed (QI)	107.00
S_v	Proposed (QI)	107.00
[12]	Eisenstein Integers	106.75
[17]	Elliptic Curve	104.00
[3]	Chaotic Map	104.70
[5]	Gaussian Integers	106.50

360 found in existing literature.

Table 5: BIC of S_s

0.0	0.5371	0.4785	0.4980	0.5020	0.4922	0.5000	0.5137
0.5371	0.0	0.4844	0.5332	0.5020	0.5156	0.4902	0.5000
0.4785	0.4844	0.0	0.4824	0.4883	0.4922	0.5137	0.4902
0.4980	0.5332	0.4824	0.0	0.4805	0.4863	0.5117	0.4980
0.5020	0.5020	0.4883	0.4805	0.0	0.5039	0.5020	0.5059
0.4922	0.5156	0.4922	0.4863	0.5039	0.0	0.4824	0.4980
0.5000	0.4902	0.5137	0.5117	0.5020	0.4824	0.0	0.5000
0.5137	0.5000	0.4902	0.4980	0.5059	0.4980	0.5000	0.0

Table 6: BIC of S_v

0.0	0.5371	0.4785	0.4980	0.5020	0.4922	0.5000	0.5137
0.5371	0.0	0.4844	0.5332	0.5020	0.5156	0.4902	0.5000
0.4785	0.4844	0.0	0.4824	0.4883	0.4922	0.5137	0.4902
0.4980	0.5332	0.4824	0.0	0.4805	0.4863	0.5117	0.4980
0.5020	0.5020	0.4883	0.4805	0.0	0.5039	0.5020	0.5059
0.4922	0.5156	0.4922	0.4863	0.5039	0.0	0.4824	0.4980
0.5000	0.4902	0.5137	0.5117	0.5020	0.4824	0.0	0.5000
0.5137	0.5000	0.4902	0.4980	0.5059	0.4980	0.5000	0.0

Table 7: BIC of S_v

S-boxes	Maximum	Minimum	Average
S_s	0.609	0.391	0.499
S_v	0.609	0.391	0.499
[12]	0.625	0.391	0.502
[17]	0.543	0.473	0.503
[13]	0.609	0.375	0.505

361 **4.3. Strict Avalanche Criterion**

362 The strict avalanche criterion of S-boxes over quaternion integers is a key property
 363 for high diffusion and cryptographic attack resistance. For the S-box to be used in SAC,
 364 the change from the input, as tiny as flipping a single bit, should lead to about a 50%
 365 change of the output bits; i.e., it should be highly unpredictable. The real part of quater-
 366 nion elements is applied to the scalar S-box in quaternion-based scale S-box design by
 367 using modular transformations and affine mapping, so that the scalar S-box retains strong
 368 avalanche property in the scalar domain. On the contrary, the vector S-box works on the

independent imagination component separately, and doing so independently of its transformations, such as modular exponentiation, rotation-based diffusion, and non-affine permutations, in order to maximize the number of bit transitions induced from input changes. The quaternion structure, however, develops an inherent way of enhancing SAC compliance due to multidimensional transformations encasing the effects of each single bit flip over both scalar and vector components, resulting in a much greater global flow of outputs. This property greatly contributes to security since it makes it impossible for attackers to establish predictable relationships between input and output values. Quaternion-based cryptographic systems are said to meet SAC requirements, so that they ensure the scalar and vector S-boxes are resistant to differential and linear cryptanalysis and therefore are appropriate cryptographic systems for use in encryption, block ciphers, and other types of advanced cryptographic systems [12, 13, 17]. Tables 8, 9 and 10 compare the proposed results to existing literature via SAC.

Table 8: SAC of S_s

0.53125	0.546875	0.5	0.5625	0.484375	0.546875	0.46875	0.515625
0.46875	0.4375	0.515625	0.515625	0.484375	0.53125	0.46875	0.546875
0.546875	0.4375	0.515625	0.46875	0.59375	0.484375	0.4375	0.5
0.53125	0.484375	0.515625	0.53125	0.5	0.546875	0.46875	0.5
0.515625	0.421875	0.5	0.5625	0.46875	0.515625	0.46875	0.5
0.515625	0.546875	0.5	0.5	0.546875	0.40625	0.484375	0.5
0.5625	0.515625	0.5625	0.5	0.484375	0.453125	0.5	0.53125
0.484375	0.53125	0.546875	0.421875	0.53125	0.53125	0.453125	0.46875

Table 9: SAC of S_v

0.53125	0.546875	0.5	0.5625	0.484375	0.546875	0.46875	0.515625
0.46875	0.4375	0.515625	0.515625	0.484375	0.53125	0.46875	0.546875
0.546875	0.4375	0.515625	0.46875	0.59375	0.484375	0.4375	0.5
0.53125	0.484375	0.515625	0.53125	0.5	0.546875	0.46875	0.5
0.515625	0.421875	0.5	0.5625	0.46875	0.515625	0.46875	0.5
0.515625	0.546875	0.5	0.5	0.546875	0.40625	0.484375	0.5
0.5625	0.515625	0.5625	0.5	0.484375	0.453125	0.5	0.53125
0.484375	0.53125	0.546875	0.421875	0.53125	0.53125	0.453125	0.46875

4.4. Linear Approximation Probability

Linear Approximation Probability (LAP) of S-boxes over quaternion integers over scalar and vector domains separately is an important measure to resist linear cryptanalysis such that the linear relation between input and output bits is not easily exploitable. Another thing is the efficiency of the attacks — the lower the LAP value, the higher the probability that no linear equation will fit the S-box accurately; therefore, the attacks

Table 10: SAC Comparison

S-boxes	Maximum	Minimum	Average
S_s	0.594	0.406	0.503
S_v	0.594	0.406	0.503
[12]	0.578	0.375	0.502
[17]	0.610	0.422	0.516
[13]	0.594	0.406	0.504

388 remain ineffectual. In quaternion-based S-box construction, the scalar S-box is designed
 389 by doing modular arithmetic and doing affine transformation on the real part of the
 390 quaternion so that the correlations between input and output are still nonlinear. To
 391 further reduce the linear dependencies, the imaginary components are transformed through
 392 independent transformations like modular exponentiation and rotation-based diffusion, as
 393 well as non-affine mappings using vector S-boxes. The nonlinearity of S-boxes is naturally
 394 improved using a quaternion structure, where the sweeping transformations over multiple
 395 dimensions increase the degree of randomness in the linearity of the approximation. An
 396 overall cryptographic system is ensured of stronger security through the low LAP of the
 397 scalar and vector S-boxes, which helps resist the linear cryptanalysis. That being said,
 398 S-boxes based on quaternions have a high suitability in encryption schemes, block ciphers,
 399 and other cryptographic applications that utilize those characteristics to keep the data
 400 safe [12, 13, 17]. Table 11 is the comparison between the proposed work and existing
 401 literature regarding the LAP.

Table 11: LAP Comparison

S-boxes	LAP
S_s	0.141
S_v	0.141
[12]	0.133
[17]	0.148
[13]	0.133

402 4.5. Differential Approximation Probability

403 Differential Approximation Probability (DAP) of S-boxes over quaternion integers is
 404 a key security parameter that characterizes their resistance against differential cryptanal-
 405 ysis by measuring the probability of occurring predictable output differences for which
 406 one determines some specific input differences. The strong diffusion required of the S-
 407 box is guaranteed by a lower DAP value, so that the transformation process could be
 408 relatively hard to trace for the attackers. In quaternion-based S-box design, the scalar
 409 S-box is built by modular arithmetic and affine mappings on the real component so as
 410 the input changes by a small bit, the output turns out to be very unpredictable. Just

411 as the vector S box processes the imaginary components, it uses independent transforma-
 412 tions like modular exponentiation, rotation-based diffusion, and non-affine permutations
 413 and applies those extremely unpredictable differential transitions. The quaternion alge-
 414 bra naturally improves the diffusion properties of S-boxes by distributing transformation
 415 in multi-dimensional space in such a way that differences in the input tokens propagate
 416 through a very complex and highly nonlinear process. Quaternion-based cryptographic
 417 systems independently optimize the scalar as well as vector parts to incorporate mini-
 418 mal DAP values and hence provide superior resistance against differential attacks, making
 419 them ideal for use in the encryption algorithms, block ciphers, and secure communication
 420 algorithms that need strong confusion and diffusion to guarantee data security [12, 14, 17].
 421 Literature comparison through Tables 12, 13, and 14 is done with the proposed results.

Table 12: DAP of S_s

0.02344	0.03125	0.02344	0.03125	0.02344	0.03125	0.02344	0.03125	0.02344	0.02344	0.02344	0.02344	0.02344	0.02344	0.03906	0.03125
0.03906	0.02344	0.03125	0.03125	0.03125	0.01562	0.02344	0.02344	0.02344	0.02344	0.02344	0.01562	0.02344	0.02344	0.02344	0.03125
0.02344	0.02344	0.03125	0.02344	0.03125	0.02344	0.02344	0.02344	0.03125	0.03125	0.03125	0.03125	0.03125	0.02344	0.03125	0.02344
0.02344	0.03125	0.03125	0.02344	0.02344	0.02344	0.03125	0.02344	0.02344	0.02344	0.02344	0.02344	0.02344	0.02344	0.03125	0.02344
0.03906	0.02344	0.02344	0.02344	0.03125	0.02344	0.02344	0.02344	0.03125	0.03125	0.03125	0.03125	0.02344	0.01562	0.02344	0.03125
0.03125	0.02344	0.02344	0.04688	0.02344	0.03125	0.03906	0.02344	0.02344	0.02344	0.02344	0.02344	0.02344	0.02344	0.02344	0.02344
0.02344	0.03125	0.03125	0.02344	0.02344	0.02344	0.03125	0.01562	0.02344	0.02344	0.02344	0.02344	0.02344	0.02344	0.02344	0.03125
0.02344	0.02344	0.02344	0.02344	0.02344	0.03125	0.02344	0.03125	0.02344	0.04688	0.03125	0.02344	0.03125	0.03125	0.02344	0.02344
0.03125	0.02344	0.01562	0.02344	0.02344	0.02344	0.03125	0.02344	0.03125	0.02344	0.03125	0.02344	0.02344	0.02344	0.03906	0.02344
0.02344	0.02344	0.02344	0.02344	0.03125	0.02344	0.02344	0.03125	0.02344	0.03125	0.03125	0.03125	0.02344	0.02344	0.03125	0.02344
0.03125	0.02344	0.03125	0.03125	0.03125	0.02344	0.02344	0.02344	0.02344	0.03906	0.02344	0.03125	0.03125	0.03125	0.02344	0.02344
0.03125	0.02344	0.03906	0.03125	0.02344	0.03125	0.03125	0.03125	0.02344	0.03125	0.02344	0.02344	0.02344	0.03125	0.03125	0.03125
0.03125	0.02344	0.02344	0.03125	0.03125	0.02344	0.03125	0.02344	0.02344	0.02344	0.03125	0.03125	0.02344	0.02344	0.03125	0.02344
0.02344	0.03125	0.02344	0.02344	0.03125	0.02344	0.02344	0.03906	0.03125	0.03125	0.03125	0.03125	0.02344	0.03125	0.03906	0.02344
0.03125	0.03125	0.02344	0.02344	0.03125	0.03906	0.02344	0.02344	0.02344	0.02344	0.02344	0.02344	0.03125	0.03906	0.02344	0.02344

Table 13: DAP of S_v

0.02344	0.03125	0.02344	0.03125	0.02344	0.03125	0.02344	0.03125	0.02344	0.02344	0.02344	0.02344	0.02344	0.02344	0.03906	0.03125
0.03906	0.02344	0.03125	0.03125	0.03125	0.01562	0.02344	0.02344	0.02344	0.02344	0.02344	0.01562	0.02344	0.02344	0.02344	0.03125
0.02344	0.02344	0.03125	0.02344	0.03125	0.02344	0.02344	0.02344	0.03125	0.03125	0.03125	0.03125	0.03125	0.02344	0.03125	0.02344
0.02344	0.03125	0.03125	0.02344	0.02344	0.02344	0.03125	0.02344	0.02344	0.02344	0.02344	0.02344	0.02344	0.02344	0.03125	0.02344
0.03906	0.02344	0.02344	0.02344	0.03125	0.02344	0.02344	0.02344	0.03125	0.03125	0.03125	0.03125	0.03125	0.02344	0.01562	0.02344
0.03125	0.02344	0.02344	0.04688	0.02344	0.03125	0.03906	0.02344	0.02344	0.02344	0.02344	0.02344	0.02344	0.02344	0.02344	0.02344
0.02344	0.03125	0.03125	0.02344	0.02344	0.02344	0.03125	0.01562	0.02344	0.02344	0.02344	0.02344	0.02344	0.02344	0.02344	0.03125
0.02344	0.02344	0.02344	0.02344	0.02344	0.03125	0.02344	0.03125	0.02344	0.04688	0.03125	0.02344	0.03125	0.03125	0.02344	0.02344
0.03125	0.02344	0.01562	0.02344	0.02344	0.02344	0.03125	0.02344	0.03125	0.02344	0.03125	0.03125	0.02344	0.02344	0.03906	0.02344
0.02344	0.02344	0.02344	0.02344	0.03125	0.02344	0.02344	0.03125	0.02344	0.03125	0.03125	0.02344	0.02344	0.02344	0.03125	0.02344
0.03125	0.02344	0.03125	0.03125	0.03125	0.02344	0.02344	0.02344	0.03125	0.02344	0.03906	0.02344	0.03125	0.03125	0.02344	0.02344
0.03125	0.02344	0.03906	0.03125	0.02344	0.03125	0.03125	0.03125	0.02344	0.03125	0.02344	0.02344	0.02344	0.02344	0.03125	0.03125
0.03125	0.02344	0.02344	0.03125	0.03125	0.02344	0.02344	0.03125	0.02344	0.02344	0.03125	0.03125	0.02344	0.02344	0.03125	0.02344
0.02344	0.03125	0.02344	0.02344	0.03125	0.02344	0.02344	0.02344	0.03125	0.03125	0.03125	0.02344	0.03125	0.02344	0.03125	0.02344
0.03125	0.03125	0.02344	0.02344	0.03125	0.03906	0.02344	0.02344	0.02344	0.02344	0.02344	0.02344	0.03125	0.03906	0.02344	0.03125

Table 14: DAP Comparison

S-boxes	DAP
S_s	0.047
S_v	0.047
[12]	0.039
[17]	0.047
[14]	0.039

422 4.6. Fixed Points

423 A fixed point of a function f is an element x in the domain such that $f(x) = x$.
424 This may provide an exploitable foundation for cryptographic systems, allowing attack-
425 ers to exploit predictable mappings. In quaternion-based S-Box implementation, where
426 scalar and vector parts are separately processed, certain careful choices of modular trans-
427 formation and affine mapping result in minimal numbers of fixed-point occurrences. A
428 nonlinear transformation of the scalar S box derived from the real part of quaternion inte-
429 gers is performed to vastly diversify the outputs. Just like the vector S-box dealing with
430 the imaginary components, it applies independent modular exponentiation and rotation-
431 based transformations to break the direct input-to-output relationships that may exist.
432 Eliminating or reducing fixed points by introducing quaternion-based S-boxes, security
433 can be improved in the sense that they are more resistant to algebraic attacks and can be
434 applied elsewhere in encryption schemes and secure communication systems [4, 15]. The
435 fixed point's comparison is given in Table 15.

436 4.7. Differential and Linear Branch Number

437 As was stated above, the branch number of an S-box plays a crucial factor in measur-
438 ing its effectiveness in spreading input differences over the output and thus its efficiency
439 against differential and linear cryptanalysis. Increasing differential branch number (DBN)
440 guarantees a small input difference produces large output differences; thus, differential
441 attacks impose less damage. Likewise, a high linear branch number (LBN) prevents linear
442 approximation attacks by making it difficult for attackers to have a good statistical corre-
443 lation between input and output values. In quaternion-based S-box design, scalar S-box
444 maximizes these branch numbers in modulo arithmetic and affine transformations, and
445 vector S-box improves it in the same component mapping. Being inherently multidimen-
446 sional, quaternion integers provide superior confusion and diffusion as compared to usual
447 transformations that would result in even more complex complexity of these transforma-
448 tions inherently, which further enhances the cryptographic security [4, 15]. LBN and DBN
449 comparison is given in Table 15.

450 4.8. Linear Structure

451 It is the idea that when linear relations exist between input and output bits, they can
452 be used for the application of linear cryptanalysis against the encryption system. In a well-
453 designed S-box, the substitution process should be highly nonlinear and unpredictable, and
454 there should be a minimum linear structure. Non-affine transformations, modular expo-
455 nentiation and quaternion rotations on the multidimensional quaternion space are applied
456 to obtain quaternion-based S-boxes where scalar and vector parts are generated separately
457 under quaternion linear transformations without linear dependencies. The scalar S-box
458 is there to ensure the real number transformations make inimitable patterns, and the
459 vector S-box, which concerns the imaginary parts, uses independent transformations to
460 further boost the non-linearity. Quaternions-based S-boxes minimize computational cost

461 and minimize linear structure, resulting in high resistance to linear cryptanalysis, and are
 462 thus ideal for secure encryption protocols, block ciphers and other cryptographic appli-
 463 cations needing strong nonlinearity [4, 15]. The linear structure comparison is given in
 464 Table 15.

Table 15: Comparative analysis of DBN, LBN, FP, and LS

S-boxes	DBN	LBN	FP	LS
S_s	1	1	1	0
S_v	1	1	1	0
[15]	2	2	2	0
[4]	1	2	2	0

465 5. Multiple RGB Image Algorithm over Quaternion Integers

466 (i) **Input Preparation:** First, the RGB images which need to be protected are im-
 467 ported, and the encryption process starts. Images stored in the RGB color model
 468 have each pixel consisting of a combination of red, green and blue values. In order to
 469 achieve encryption, the pixel values of the image channels are mapped to elements
 470 of the quaternion integer set $H(K)_\delta$. Specifically, this mapping ensures that the
 471 encryption scheme is conducted in the quaternion domain with the dip advantage of
 472 the quaternion algebraic structure to provide enhanced security.

473 (ii) **S-Box Construction:** Using quaternion integer residue classes $H(K)_\delta$, two 8×8
 474 S-boxes are constructed S_s and S_v . The introduction of nonlinearity and complexity
 475 with these structures is important, as they enormously strengthen the encryption.
 476 The use of quaternion arithmetic has a unique set of properties that are more re-
 477 sistant to cryptographic breaking attacks than what is provided using integer-based
 478 approaches.

479 (iii) **SPN Framework:** The encryption scheme is developed in the SPN framework,
 480 and the security of multiple RGB images is improved by the following three steps:
 481 **Substitution Step:** Of the stages, the first is the Substitution Step, where the con-
 482 fusion is introduced using S-box S_s . Then substitute every one of the Red, Green,
 483 and Blue channel pixels accordingly by a substitution operation which replaces the
 484 input values with the corresponding outputs from S_s . Thus, quaternion-integer-
 485 based S-boxes allow high nonlinearity, rendering it much more difficult to carry out
 486 a study, particularly on linear and differential attacks. **Permutation Step:** The
 487 S-box S_v is used in the second stage to perform a permutation step, which improves
 488 the diffusion properties by redistributing transformed pixel values. The reordering
 489 of each RGB channel is independent of each other, eliminating substitution-induced
 490 correlations for a reduced chance for pattern detection from attackers. This process
 491 is enhanced by adding the quaternion integer domain, which increases the number

492 structure to a more complex number and disrupts statistical relations further. **Fi-**
493 **nal XOR Operation:** The generation of S' -box depends on performing an XOR
494 operation between S_s and S_v which marks the final transformation. Security reaches
495 its highest mark in the last step, which introduces additional randomization. The
496 pixel values in digital images experience an XOR operation using rendering; it is
497 impractical for hackers to perform keyless reconstruction of transformations. The
498 decryption process remains possible only through the precise encryption key that
499 was originally used in the process.

500 (iv) **Final Transformation:** Every RGB channel receives a transformation through
501 the SPN process which optimizes confusion and diffusion across the complete image.
502 The purpose of this security-enhancing step is to protect against both differential and
503 statistical attacks, thus creating an encrypted image with strong resistance against
504 unauthorized decryption attempts.

505 (v) **Output the Encrypted Image:** The implementation of all encryption methods
506 produces an encrypted RGB image which results from merging the modified red,
507 green and blue color channels. The encryption algorithm runs for all RGB images
508 contained in the dataset to deliver complete information security.

509 (vi) **Security Enhancement and Final Output:** A cryptographic process results in
510 encrypted images that present high levels of randomness through increased entropy
511 along with low pixel correlation alongside intense resilience to cryptographic anal-
512 ysis. Through quaternion integer-based encryption the framework delivers secure
513 multimedia transmission since encrypted images become significantly unpredictable
514 to both modern cryptanalysis methods and traditional cryptanalytic attacks.

515 **Significance of RGB Multiple Color Image Encryption:** Secure multimedia data
516 transmission benefits substantially from the use of quaternion integers to encrypt multi-
517 ple RGB images. Modern cryptographic attacks frequently break traditional encryption
518 methods based on real and complex numbers because these methods lack enough algebraic
519 complexity. The security benefits from quaternion integer use stem from their elevated
520 dimensional structure along with their non-commutative properties, which cause brute-
521 force attacks, linear approximations and differential cryptanalysis to become increasingly
522 difficult to perform. The main benefit of using quaternion encryption is its channel in-
523 dependence processing capability, which ensures secure image integrity by maintaining
524 dependencies across color channels and providing strong diffusion and confusion capa-
525 bilities. Quaternion residue classes integrated with substitution-permutation networks
526 (SPN) adopt mathematical methods for distributing pixel data that make them resilient
527 against statistical attacks. Nonlinearities strengthen due to the construction of secure
528 S-boxes based on quaternion integer residue classes because these results help protect
529 against cryptographic weaknesses. Quaternions enable efficient implementation of secure
530 transformations that produce encrypted images with high entropy values and reduced cor-
531 relation along with strong dependency to keys. The encryption technique delivers excep-
532 tional benefits for secure image transfer and cloud backup alongside defence needs because

533 it maintains highly confidential data while resisting attacks effectively. This encryption
 534 framework takes advantage of quaternion integers' distinct algebraic properties to develop
 535 a superior encryption system when compared to classic approaches, thus delivering better
 536 security and computation speed to actual multimedia encryption operations.
 537 Sections 3 and 4 S-box construction joins the production process with multiple RGB image
 538 encryption methods as described in Section 5 according to Figure 2.

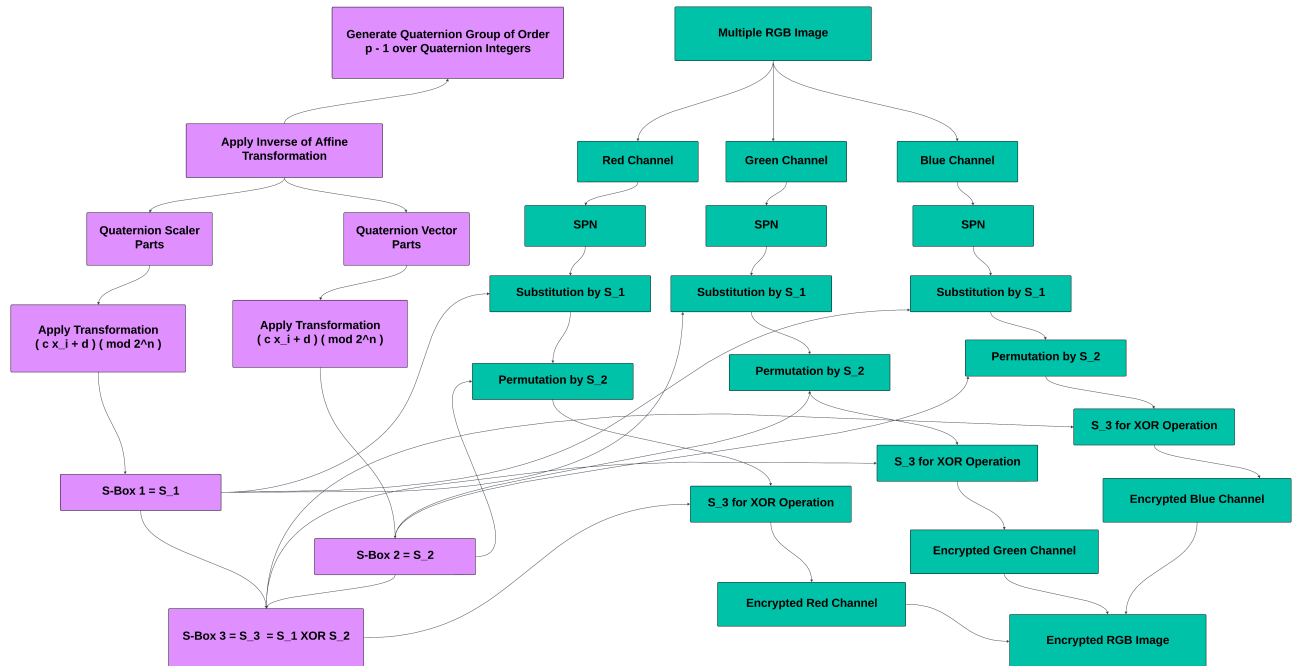


Figure 2: Flowchart of proposed study

6. Applications of Multiple RGB Image Encryption over Quaternion Integers

541 Multiple RGB image encryption over quaternion integers is a very powerful technique
 542 for encrypting the digital images in a secure way by utilizing the multidimensional prop-
 543 erties of the quaternions. Quaternions are four-dimensional, and quaternion-based en-
 544 cryptation operates over the quaternion system, which means scalar and three imagi-
 545 nary components. The increase in complexity and unpredictability of the encryption process
 546 is achieved by means of this higher-dimensional representation which is capable of complex
 547 transformation. Using this methodology, each of the RGB images is separated into their
 548 color channels, where they are then converted into quaternion space and processed with
 549 encryption using substitution-permutation networks (SPN), modular arithmetic and affine
 550 transformations, respectively, on the scalar and vector components. This involves strong
 551 diffusion and confusion, meaning that even a very modest change of the original image
 552 leads to a very different output in the encrypted version. Quaternion multiplication and

553 rotation functions allow for much more sensitivity of the system to keys, and the system is
 554 thus very resistant to brute force and statistical attacks. With this technique, the secure
 555 encryption and transmission of multiple RGB images while resisting cryptography attacks
 556 can be easily achieved; hence, this is a good technique for secure image communication,
 557 cloud saving, and multimedia security applications [5, 16, 21, 34]. Figure 3 shows two
 original multiple RGB images I_1 , and I_2 alongside their encrypted versions.

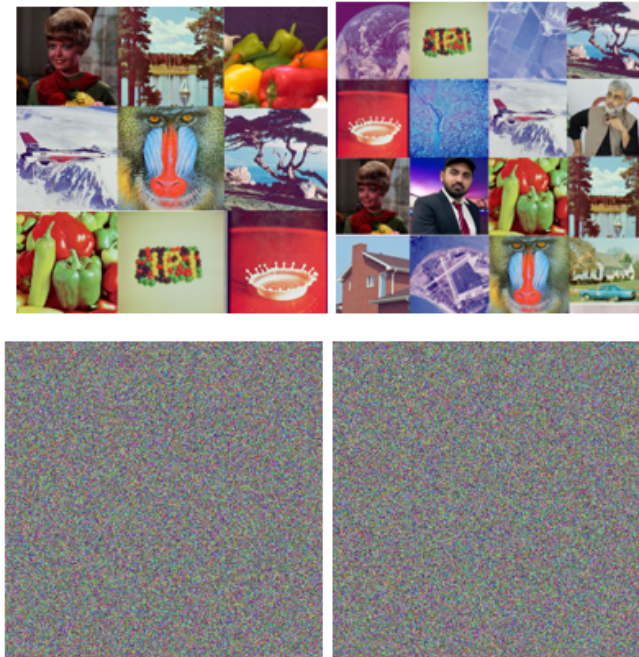


Figure 3: Quaternion integers-based multiple original and encrypted RGB images

558

559 6.1. Histogram Analysis (HA)

560 Histogram analysis is a vital method of checking the security and performance of more
 561 than one RGB image encryption utilizing quaternion integers. This analyzes the distri-
 562 bution of pixel intensity values in encrypted images to determine whether the encryption
 563 process indeed covers up all the statistical properties of the original images. In a well-
 564 encrypted image both the histogram and the power spectrum should look uniform (homo-
 565 geneously distributed across the entire intensity/density range); this blocks any detectable
 566 patterns for attackers to exploit. If we encrypt the RGB images that are in the form of
 567 quaternion integers using such an encryption algorithm, the encryption algorithm trans-
 568 forms the scalar and vector components separately based on nonlinear operations such as
 569 substitution, permutation, and quaternion multiplication. By placing constraints on indi-
 570 vidual components of a color plane of an image, this further strengthens the security of the
 571 encrypted image such that each color channel undergoes independent transformations that
 572 are still correlated. The histograms of the original and encrypted images analyzed show

573 that the proposed quaternion-based encryption breaks the pixel correlations, hence pro-
 574 ducing histograms largely similar to signatures of randomness. This randomness greatly
 575 limited the likelihood of a statistical attack based on the encrypted image since the attack-
 576 ers cannot learn any meaningful information from the encrypted image. This encryption
 577 scheme is proven effective in that the histogram of the encrypted image is entirely devoid
 578 of any resemblance to that of the original image and is strong against frequency-based
 579 cryptanalysis; hence, the images are kept confidential [5, 16, 21]. Figure 4 is the multiple
 580 original and encrypted RGB image histogram analysis.

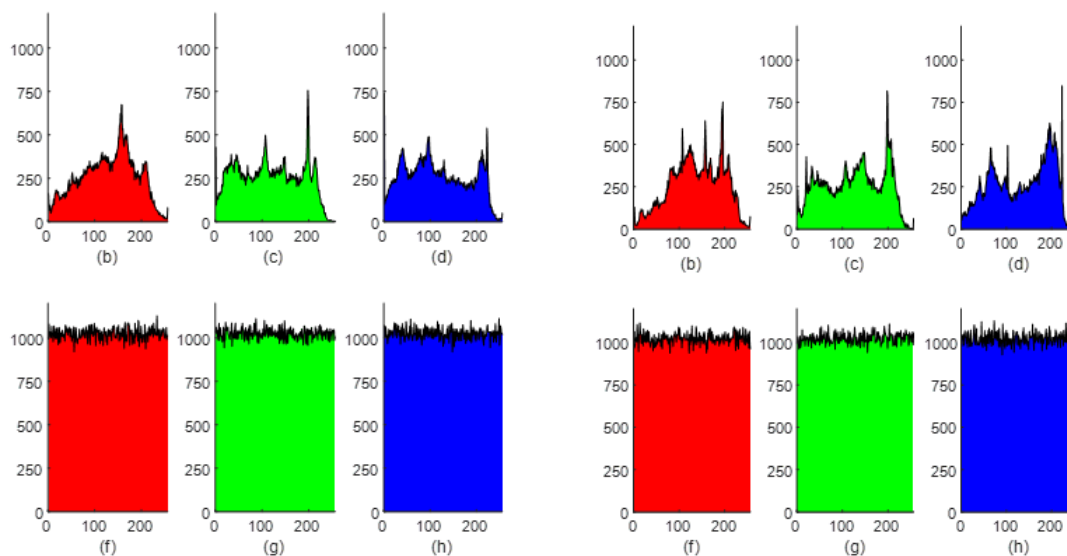


Figure 4: Histogram analysis of original and encrypted images I_1 & I_2

581 6.2. NPCR

582 In regards to multiple RGB image encryption over quaternion integers, we have a
 583 metric of key interest: the Number of Pixels Change Rate (NPCR), which measures how
 584 sensitive an encryption algorithm is to small changes in the plaintext image. The NPCR
 585 measures the percentage of pixels that are moved (changed) in the encrypted image to
 586 only one changed pixel in the original image. A higher value of NPCR indicates that
 587 the encryption process spreads minor changes over the whole encrypted image, so the
 588 changes are resistant to attacks and cannot be used to extract details from encrypted
 589 images. In quaternion-based encryption, where an RGB image is mapped to quaternion
 590 space and processed independently on scalar and vector parts, a small modification to
 591 the input causes a large alteration in the encrypted output. Quaternion multiplication,
 592 rotation-based transformations, and substitution permutation networks (SPN) are used
 593 to guarantee even a very small change in any one pixel will propagate unintelligibly into
 594 all three color channels. Therefore, an ideal quaternion-based encryption scheme achieves
 595 NPCR near to 99%, indicating that the encryption method gives a high degree of random-

596 ness and unpredictability, making it very hard to extract meaningful info from encrypted
 597 pictures for the assailants [5, 16, 21, 34]. The NPCR results are in Table 16.

598 6.3. UACI

599 The Unified Average Changing Intensity (UACI) is another important metric used to
 600 assess the use of the image encryption algorithm to measure the average intensity difference
 601 between the original and the encrypted images. Higher UACI values quantify the impact
 602 of small changes in the plaintext image on the encrypted image, i.e., the stronger the
 603 diffusion properties. For the encryption over quaternion integers in multiple RGB images,
 604 UACI is used to evaluate how efficiently the encryption spoils the overall pixel intensity
 605 distribution in different color channels. As quaternion-based encryption encrypts the scalar
 606 and vector components of an image independently and applies modular arithmetic, affine
 607 mappings, and quaternion rotations to the transformed form independent of each other,
 608 the slight changes in the input will have a large variation in pixel intensity after encryption.
 609 Using this enhanced diffusion mechanism, attackers are prevented from building statistical
 610 correlations between the encrypted and unencrypted images for security. Typically, an
 611 optimal quaternion-based encryption scheme achieves a high UACI value, indicating that
 612 the mean of change across the encrypted image is sufficiently high with substantial change
 613 in pixel intensity, which is the most important factor in resisting statistical and differential
 614 attacks [5, 16, 21, 34]. The UACI results are in Table 16.

Table 16: NPCR and UACI analysis

Images	NPCR			UACI		
	Red	Green	Blue	Red	Green	Blue
Image I_1	0.9962	0.9962	0.9961	0.2999	0.3145	0.3185
Image I_2	0.9960	0.9961	0.9963	0.2956	0.3094	0.3112
[16]	0.9960	0.9961	0.9961	0.3347	0.3347	0.3346
[21]	0.9969	0.9969	0.9966	0.3367	0.3332	0.3367
[34]	0.9961	0.9961	0.9961	0.3544	0.3177	0.3419
[5]	0.9959	0.9964	0.9962	0.3269	0.3037	0.2762

615 6.4. Maximum Deviation

616 Maximum deviation analysis is an important statistical measure for the modelling
 617 and evaluation of the randomness and effectiveness of the encryption of quaternion inte-
 618 gers into multiple RGB images. It quantifies the largest absolute difference between the
 619 pixel intensity distributions of the original and encrypted images and gives insight into
 620 how well the encryption algorithm disrupts the structural properties of the input data.
 621 The larger the maximum deviation value, the better the encryption scheme, as it im-
 622 plies that the encrypted image appears very unpredictable and significantly distinguishes
 623 from the original. Maximum deviation analysis is used to validate the diffusion capability

624 of quaternion-based encryption, and the argument is that where RGB images are trans-
 625 formed by distinct transformations on the scalar and vector parts of quaternion space,
 626 maximum deviation analysis validates the algorithm's diffusion capability. By application
 627 of quaternion multiplication, affine transformation, and, of course, nonlinear operations,
 628 the smallest fluctuation in pixel value is propagated extensively across all the color chan-
 629 nels and makes intensity distribution drastically different. Researchers also analyze the
 630 maximum deviation between histograms of the original and encryption images to verify
 631 that the proposed encryption scheme successfully removes the pattern and is not vulner-
 632 able to statistical attacks. The maximum deviation values obtained by quaternion-based
 633 encryption signify its robustness to provide secure transmission and storage of many RGB
 634 images against crypto threats [5, 34]. Table 17 provides the results obtained from MD
 635 testing.

636 6.5. Irregular Deviation

637 As an important statistical measuring method, irregular deviation of multiple RGB
 638 image encryption over quaternion integers is carried out. This analysis checks whether
 639 the histograms of the encrypted images have been regularized to an extent comparable
 640 to that of the histogram between the histogram of the original and encrypted images by
 641 the encryption algorithm and verifies that such patterns may appear in the previous im-
 642 ages. The irregular deviation value is a high value which implies that the encrypted image
 643 has some randomness, and thus attacks cannot guess anything about the image due to
 644 randomness. In the encryption process of quaternion-based encryption, the RGB images
 645 mapped in quaternion space are subjected to independent transformations on scalar and
 646 vector components, which disrupts pixel intensity distributions of all color channels. To
 647 achieve said variation, quaternion multiplication, nonlinear transformations and permu-
 648 tation substitution operations are used. By inspecting the histograms of the plaintext
 649 and ciphertext images with regard to the irregular deviation, it is shown that quaternion
 650 encryption has a very high entropy. The encryption scheme thus has an additional level of
 651 randomness that prevents statistical attacks to secure transmission and storage of multiple
 652 RGB images in cryptographic applications [5, 34]. The results regarding ID are presented
 653 in Table 17.

Table 17: MD and ID analysis

Images	NPCR			UACI		
	Red	Green	Blue	Red	Green	Blue
Image I_1 Encrypted	52021	61841	61742	38097	37989	37924
Image I_2 Encrypted	61424	62086	52113	38171	37937	38159
[34]	53397	48329	53529	29231	25127	28374
[5]	60210	47069	62218	26266	19443	27027

654 **6.6. Correlation Analysis**

655 The term evaluation metric includes correlation analysis, horizontal, vertical and di-
 656 agonal correlation in order to measure the average security of utilizing multiple RGB
 657 image encryption with quaternion integers. In an unencrypted image, neighbouring pixels
 658 are strongly correlated because natural images are full of neighbouring pixels that have
 659 similar intensity values. Nevertheless, any good encryption scheme should significantly
 660 decrease these correlations so as to render the encrypted image look like nothing but a
 661 random noise. Through quaternion-based encryption techniques, RG images are converted
 662 to quaternion space, and encryption is done independently on scalar and vector compo-
 663 nents. To ensure that neighbouring pixels in horizontal, vertical, and diagonal directions
 664 all receive individual and impossible-to-predict transformations, the process of encryption
 665 involves non-linear transformations, quaternion multiplication, and substitution permuta-
 666 tion network (SPN). Thus, although the neighbouring pixels of the encrypted image still
 667 show some correlation coefficients, they are approaching values close to zero, which means
 668 that there is no more statistical relationship between the adjacent pixels. Such reduction
 669 in correlation ensures that the encrypted image does not betray any structural information
 670 from the original image, so it is very immune to statistical attacks. Then it is found that
 671 quaternion-based encryption can significantly enhance security and thus is an effective
 672 way for secure image transmission and storage by comparing the horizontal, vertical and
 673 diagonal correlations before and after encryption [5, 16, 21, 34]. The correlation analysis
 674 is given in Figure 5 and 6 with Table 18 data.

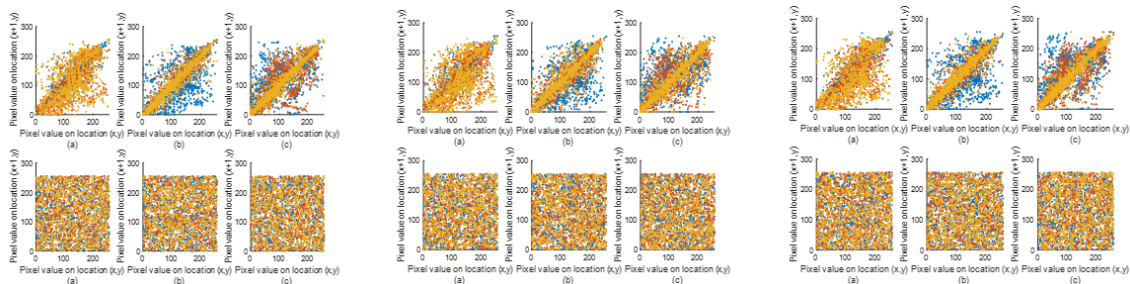


Figure 5: Vertical, diagonal and horizontal correlation analysis of image I_1

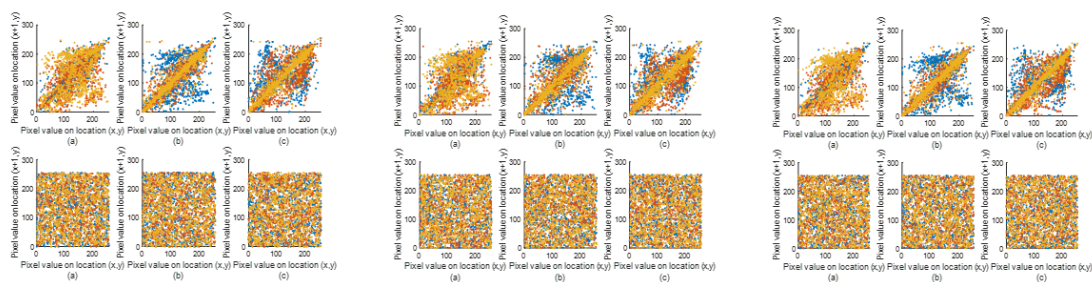


Figure 6: Vertical, diagonal and horizontal correlation analysis of image I_2

Table 18: Vertical, diagonal and horizontal correlation analysis of different images

Images		Vertical			Diagonal			Horizontal		
		Red	Green	Blue	Red	Green	Blue	Red	Green	Blue
Image I_1 Original	Red	0.9340	0.7323	0.5096	0.9038	0.6895	0.5161	0.9235	0.7030	0.5486
	Green	0.5420	0.9474	0.9431	0.5494	0.9068	0.9054	0.5506	0.9410	0.9388
	Blue	0.5423	0.7284	0.9462	0.5679	0.7200	0.8945	0.5530	0.7589	0.9408
Image I_1 Encrypted	Red	-0.0400	0.0067	-0.0234	-0.0026	0.0017	0.0312	0.0284	0.0115	0.0365
	Green	0.0462	-0.0158	0.0145	-0.0186	0.0074	-0.0144	0.0040	-0.0168	0.0035
	Blue	0.0306	0.0039	-0.0308	-0.0472	-0.0077	0.0103	-0.0190	0.0102	0.0321
Image I_2 Original	Red	0.8956	0.6007	0.3919	0.8669	0.5082	0.3964	0.9201	0.6211	0.3671
	Green	0.3843	0.9275	0.9250	0.3603	0.8285	0.9071	0.3508	0.9142	0.9258
	Blue	0.3805	0.7224	0.9174	0.3655	0.7086	0.8968	0.3911	0.7223	0.9323
Image I_2 Encrypted	Red	-0.0027	-0.0324	0.0205	-0.0136	0.0149	0.0055	0.0033	-0.0675	-0.0665
	Green	0.0164	-0.0081	-0.0133	-0.0217	-0.0512	0.0539	-0.0260	0.0179	0.0124
	Blue	0.0425	-0.0180	0.0351	0.0162	-0.0239	0.0115	0.0013	-0.0432	-0.0107

6.7. Information Entropy

It is an important figure of speech for multiple RGB image encryption over quaternion integers and randomness and security. It is the measure of uncertainty of the encrypted image; in an ideal encryption scheme, the entropy value for such an image with 8 bits of greyscale or color should be close to 8, thus indicating a uniform distribution of pixel intensities. In quaternion-based encryption, RGB images are mapped to quaternion space, followed by the independent transformation of scalar and vector components of each image according to substitution, permutation, quaternion multiplication and modular arithmetic. Therefore, these processes make the pixel intensity values of the encrypted image distributed as randomly as possible, without having any inherent patterns of the original image. A large entropy value indicates that the image content is well obfuscated by the encryption method, and he or she is highly resistant to statistical attack, information leakage and cryptanalysis. The entropy of the image if considerably lower than 8 implies that the image carries redundant information which could be used by the attackers to deduce the original image. The quaternion-based encryption achieves entropy values close to the theoretical maximum, thereby securing the encrypted multiple RGB images by creating the maximum randomness for transmission and storage in cryptographic applications [5, 16, 35]. A comparison of the proposed work's entropy evaluation is made to the existing research noted in Table 19.

Table 19: Information Entropy comparison

Images	Information Entropy			Average
	Red	Green	Blue	
Image I_1	7.9992	7.9994	7.9993	7.9993
Image I_2	7.9993	7.9994	7.9992	7.9993
[16]	7.9913	7.9914	7.9916	7.9916
[35]	7.9888	7.9896	7.9890	7.9892
[21]	7.9995	7.9995	7.9994	7.9995
[5]	7.9976	7.9967	7.9976	7.9987

694 **6.8. MSE**

695 Mean Squared Error (MSE) is employed to compare the original encrypted images in
 696 multiple RGB image encryption over quaternion integers. The MSE quantifies the average
 697 squared differences between the corresponding pixel intensities, and the higher values of
 698 MSE mean that stronger encryption is achieved through ensuring a significant deviation
 699 from the original image. In a quaternion-based encryption, i.e., transforming images to
 700 quaternion space to allow scalar and vector components of each pixel to be independently
 701 processed by substitution, permutation, and quaternion multiplication operations, in the
 702 quaternion-based encryption process, the pixel intensity variation is maximized. For a well-
 703 designed encryption scheme, the MSE measures should be high such that the encrypted
 704 image has no similarity to the original one, which makes the image resistant to visual
 705 attacks as well as statistical analysis. On the one hand, quaternion-based encryption with
 706 large MSE values both guarantees good diffusion and confusion so as to avoid attackers
 707 obtaining any meaningful pattern or reconstructing the original image [34]. The data
 708 collected MSE are given in Table 20.

709 **6.9. PSNR**

710 The Peak Signal to Noise Ratio (PSNR) is an important metric to evaluate the qual-
 711 ity degradation between the original encrypted images in many RGB image encryptions
 712 over quaternion integers. PSNR inversely relates to MSE, and a lower PSNR means the
 713 encryption has better performance, meaning that the encrypted image is much distorted
 714 and can't be recognized from the original. Since quaternion-based encryption is an inde-
 715 pendent transformation of the scalar and vector components of an image using nonlinear
 716 and algebraic operations, it increases pixel randomness and hence reduces the PSNR value
 717 significantly. The lower PSNR indicates that the encrypted image went through extreme
 718 modifications, and those kinds of modifications would be beyond the capability for attack-
 719 ers to decode the original image by means of standard signal processing. PSNR values are
 720 found to be low, also indicating that the encryption is effective in validating the encryp-
 721 tion's robustness and the resistance to inverse attacks [34]. Table 20 contains the collected
 722 PSNR and MSE data.

Table 20: MSE and PSNR analysis

Images	MSE			PSNR		
	Red	Green	Blue	Red	Green	Blue
Image I_1 Original	2.50	2.33	2.53	44.1849	44.4965	44.1297
Image I_1 Encrypted	2.54	2.48	2.38	44.1080	44.2180	44.3952
Image I_2 Original	2.53	2.62	2.48	44.1320	43.9747	44.2144
Image I_2 Encrypted	2.44	2.53	2.36	44.2969	44.1377	44.4353
Original Image [34]	2.23	2.47	2.10	44.6746	44.2313	44.9505
Encrypted Image [34]	2.43	2.42	2.38	44.3020	44.3185	44.4057

723 **6.10. Contrast**

724 The parameter of multiple RGB image encryption over quaternion integers is contrast
 725 analysis, which is the difference of intensity between two adjacent pixels. To prevent
 726 the encrypted image from displaying any identifiable features of the plaintext image, the
 727 original contrast levels of the plaintext image should be disrupted by encrypting them in
 728 a secure encryption algorithm. Quaternion encryption provides an additional source of
 729 randomness and distorts the contrast distribution by mapping RGB images to quaternion
 730 space and performing independent transformations of the scalar and vector components.
 731 Encryption with strong encryption is indicated by high intensity currents in the encrypted
 732 image by eliminating the structural consistency and the sensitivity to statistical attacks.
 733 The encrypted images should have their contrast values that do not correlate with those
 734 of the original images to ensure secure image transmission and storage as well [21, 34].
 735 Table 21 presents the result of contrast evaluation in the proposed work.

736 **6.11. Energy**

737 Energy is a texture analysis measure to determine if pixel intensity distribution in
 738 the image is one of repetitive pattern (with a high value) or random (with a low value).
 739 The purpose of multiple RGB image encryption over quaternion integers is to obtain an
 740 energy value of a disordered and unpredictable pixel distribution. The quaternion based
 741 encryption is built upon substitution permutation networks (SPN), quaternion multipli-
 742 cation and nonlinear transformation mechanisms to disrupt original energy distribution
 743 such that encrypted image is with a uniform and random texture. The encryption process
 744 is effective if there is a significant deviation in energy values between the original and en-
 745 crypted images and therefore no recognizable patterns can be exploited by the attackers.
 746 By thoroughly encrypting an image, its energy value to its plaintext counterpart should be
 747 drastically different, as a confirmation that encryption can perform visual data obfuscation
 748 [21, 34]. The presented energy data is shown in Table 21.

Table 21: Contrast and energy analysis

Images	Contrast			Energy		
	Red	Green	Blue	Red	Green	Blue
Image I_1 Original	0.5693	0.6411	0.6196	0.0752	0.0735	0.0713
Image I_1 Encrypted	10.5357	10.4913	10.4710	0.0156	0.0156	0.0156
Image I_2 Original	0.6062	0.7930	0.6063	0.0828	0.0748	0.0906
Image I_2 Encrypted	10.4667	10.5053	10.5311	0.0156	0.0156	0.0156
Original Image [21]	0.5439	0.5000	0.4726	0.5439	0.5000	0.4726
Encrypted Image [21]	10.5114	10.4770	10.4894	10.5114	10.4770	10.4894
Original Image [34]	0.4717	0.4879	0.4261	0.0838	0.0834	0.1242
Encrypted Image [34]	10.4878	10.4861	10.5034	0.0156	0.0156	0.0156

749 6.12. Statistical Homogeneity

750 Statistical homogeneity relates to the uniformity of a gray image's texture and is de-
 751 termined based on successive pixel intensities. For the scheme of multiple RGB image en-
 752 cryption over quaternion integers, it needs to break pixel similarity so that the encrypted
 753 image will be more homogenous. Quaternion based encryption does this by separately
 754 transforming the scalar and vector part of each pixel by modular arithmetic, affine trans-
 755 formation, and quaternion rotation. These transformations also bring randomness thus
 756 neighboring pixels of encrypted image not related in any steady way. A lower homogene-
 757 ity value in the encrypted image means the encryption algorithm adversely disturbs the
 758 structural consistency of the image rendering it very indomitable to statistical as well as
 759 differential attacks. The security of quaternion based encryption is enhanced because it
 760 reduces homogeneity and the encrypted image cannot be meaningfully extracted by the
 761 attacker [34]. The results of the proposed work for homogeneity are presented in Table
 762 22.

763 6.13. Standard Deviation

764 The SD is a necessary statistical index for the evaluation of dispersion of pixel inten-
 765 sities in multiple RGB image encryption over quaternion integers. The greater the value
 766 of an encrypted image's SD, the broader the spread of pixel intensities, since this indi-
 767 cates a strong encryption process that has removed all patterns and correlations present
 768 in the original image. Quaternion based encryption uses separate scalar and vector com-
 769 ponents upon which they interleave nonlinear transforms, quaternion multiplication and
 770 permutation-substitution networks in order to distribute pixel values uniformly across
 771 color channels. This dispersion is required for achieving a very high randomness in the
 772 encrypted image so it can be resistant to statistical attacks. If the chosen encryption
 773 process is secure, we should observe a greatly different SD between the original and the
 774 encrypted images, which ensures that the encryption has successfully masked the struc-
 775 tural consistency. Through a high SD, quaternion based encryption not only increases
 776 security for multiple RGB images, but prevents these images from being decrypted or
 777 pattern recognized by any unauthorized user [34]. Table 22 shows a description of the SD
 778 test results of the proposed work.

Table 22: Homogeneity and standard deviation

Images	Homogeneity			Standard Deviation		
	Red	Green	Blue	Red	Green	Blue
Image I_1 Original	0.8335	0.8324	0.8293	57.4332	64.5652	65.8041
Image I_1 Encrypted	0.3891	0.3892	0.3899	73.8951	73.9193	73.9622
Image I_2 Original	0.8384	0.8198	0.8499	54.7737	63.0304	63.5231
Image I_2 Encrypted	0.3801	0.3897	0.3897	73.9140	73.8647	73.9488
Original Image [34]	0.8855	0.8726	0.8855	9.5315×10^3	8.5820×10^3	1.0732×10^4
Encrypted Image [34]	0.3892	0.3897	0.3889	72.3821	67.0023	61.9652

6.14. NIST Test

779 **6.14. NIST Test**
780 Randomness of quaternion integer multiple RGB image encryption: The NIST sta-
781 tistical test suite is a standard method for testing random and security strength of the
782 encryption scheme, especially for the multiple RGB image encryption over integers. This
783 suite exercises several tests of various aspects of randomness to check that the encrypted
784 images have highly unpredictable pixel distributions. Frequency test is used to deter-
785 mine that whether the amount of ones and zeros in the encrypted image is the same and
786 therefore the randomness is uniform. However, the block frequency test expands this idea
787 by analyzing certain blocks in the encrypted image, ensuring that there is randomness
788 maintained between segments of the encrypted image. The rank test ensures that the
789 encryption breaks down structured relationships of values in the image, and the linear
790 dependence is examined between pixel values. The runs test (M=10,000) and long runs of
791 Ones test check for the consistency of sequences of like pixel values, and there is no resid-
792 ual of predictable pattern. Repeated patterns are analyzed in the overlapping templates
793 and non-overlapping templates tests, which verify that quaternion based encryption would
794 result in a large variability over the image. The spectral DFT tests evaluate the encrypted
795 data on periodic structures, which prevents the frequency based attacks since it should not
796 contain the dominating spectrum. The complexity of pixel arrangements is estimated by
797 the approximate entropy test and thus verifies that the encrypted image has an irregular
798 unpredictable structure. The universal test is a test if the encrypted image has compress-
799 ible patterns with high randomness, and thus is resistant to redundancy-based attacks.
800 The serial tests determine the independence of pixel transitions, that pixels are not next
801 to each other and follow any pattern. The cumulative sum tests (forward and reverse)
802 include tests that verify the uniformity of pixel distribution across the encrypted image
803 without any directional biases. Random excursions and random excursions variants tests
804 evaluate the randomness of the trajectory of pixel value sequence to ensure that quater-
805 nion based encryption successfully destroys patterns and continues to be unpredictable.
806 Multiple methods of RGB image encryption over quaternion integers then pass these NIST
807 tests and show robustness to securing image data, resisting statistical, differential and fre-
808 quency based cryptanalysis techniques [34, 36]. NIST evaluates its results through Table
809 23.

Table 23: NIST analysis of encrypted image I_1

Tests		P-values			Remarks
		Red	Green	Blue	
Frequency		0.72795	0.52709	0.84952	✓
Block frequency		0.8214	0.94307	0.64453	✓
Rank		0.29191	0.29191	0.29191	✓
Runs (M=10,000)		0.29579	0.52292	0.020941	✓
Long runs of ones		0.7127	0.7127	0.7127	✓
Overlapping templates		0.85988	0.85988	0.81567	✓
No overlapping templates		1	0.9994	0.99981	✓
Spectral DFT		0.14679	0.77167	0.11048	✓
Approximate entropy		0.90625	0.35541	0.5992	✓
Universal		0.99668	0.98733	0.99844	✓
Serial	p values 1	0.55822	0.020917	0.030786	✓
Serial	p values 2	0.64206	0.0036093	0.92887	✓
Cumulative sums forward		0.224	0.24591	0.24146	✓
Cumulative sums reverse		0.96051	0.88005	1.0587	✓
Random excursions	X = -4	0.15244	0.30689	0.13725	✓
	X = -3	0.23199	0.46172	0.21775	✓
	X = -2	0.10689	0.25688	0.0091833	✓
	X = -1	0.83873	0.71524	0.83249	✓
	X = 1	0.82206	0.62668	0.63515	✓
	X = 2	0.052698	0.0055571	0.3526	✓
	X = 3	0.60677	0.28872	0.26048	✓
	X = 4	0.12628	0.2527	0.58195	✓
Random excursions variants	X = -5	0.7473	0.89286	0.98091	✓
	X = -4	0.89103	0.93913	0.82814	✓
	X = -3	0.95691	0.92801	0.46022	✓
	X = -2	0.91666	0.81554	0.40709	✓
	X = -1	0.67238	0.2665	0.61527	✓
	X = 1	0.46848	0.68617	0.61527	✓
	X = 2	0.23567	0.86111	0.90103	✓
	X = 3	0.19469	0.75183	0.74815	✓
	X = 4	0.22621	0.76003	0.37052	✓
	X = 5	0.28584	0.89286	0.48767	✓

7. Discussion, Conclusion, and Future Work

810

811 This paper proposes a novel encryption scheme for different ways of combining mul-
 812 tiple RGB images which are secured by Substitution-Permutation Network (SPN)-based
 813 encryption scheme for quaternion integers. Using the mathematical properties of the
 814 quaternions integers, specifically their four dimension, the proposed method increases the

815 cryptographic strength of S-boxes, consequently improving nonlinearity, confusion, and
816 diffusion properties. Using quaternion integer based S boxes in conjunction with an SPN
817 based encryption scheme gives high security level, protected from attack by statistical,
818 differential and cryptanalytic attacks. Furthermore, the proposed algorithm is computa-
819 tionally efficient, which allows for real time applications in domains where secure mul-
820 timedia transmission in cloud storage, medical imaging, and such are progressing. The
821 presented encryption framework is tested through extensive theoretical and experimental
822 analysis and is proved to be resilient and practical compared to the conventional methods.
823 Computational complexity in the future research can be optimized, other cryptographic
824 primitives can be extended by the approach, and the applicability in resource constrained
825 environment can be further explored for enhancing the digital security in modern multi-
826 media applications.

827 The optimization of computational complexity of quaternion integer based encryption
828 schemes for real time application can be one future research. These larger and more com-
829 plex algebraic structures offer further security benefits including exploration of octonion
830 or sedenion integers. It is possible to broaden the applicability of the proposed framework
831 to other cryptographic primitives such as hash functions and digital signatures. Working
832 together with the latest technologies like quantum cryptography and lightweight crypto-
833 graphic protocols for IoT and edge computing, the process of encryption may be integrated
834 and this would serve as a lot of help in having a good digital security in different uses.

835 Acknowledgements

836 The Researchers would like to thank the Deanship of Graduate Studies and Scientific
837 Research at Qassim University for financial support (QU-APC-2025).

838 Data availability

839 The images used in this study were obtained from 'The USC-SIPI Image Database'
840 (<https://sipi.usc.edu/database>). The images were combined and processed to meet the
841 specific pixel requirements of the experiment. The researcher can contact to the Muham-
842 mad Sajjad for getting the images.

843 References

- 844 [1] Alfred J Menezes, Paul C Van Oorschot, and Scott A Vanstone. *Handbook of applied*
845 *cryptography*. CRC press, 2018.
- 846 [2] Claude Carlet and Cunsheng Ding. Nonlinearities of s-boxes. *Finite fields and their*
847 *applications*, 13(1):121–135, 2007.
- 848 [3] Majid Khan, Tariq Shah, Hasan Mahmood, Muhammad Asif Gondal, and Iqtadar
849 Hussain. A novel technique for the construction of strong s-boxes based on chaotic
850 lorenz systems. *Nonlinear Dynamics*, 70:2303–2311, 2012.

- 851 [4] Naveed Ahmed Azam, Umar Hayat, and Maria Ayub. A substitution box generator,
852 its analysis, and applications in image encryption. *Signal Processing*, 187:108144,
853 2021.
- 854 [5] Muhammad Sajjad, Tariq Shah, Tanveer ul Haq, Bander Almutairi, and Qin Xin.
855 Spn based rgb image encryption over gaussian integers. *Heliyon*, 10(9), 2024.
- 856 [6] Giuliana P Davidoff, Peter Sarnak, and Alain Valette. *Elementary number theory,*
857 *group theory, and Ramanujan graphs*, volume 55. Cambridge university press Cam-
858 bridge, 2003.
- 859 [7] Muhammad Sajjad and Tariq Shah. Decoding of cyclic codes over quaternion integers
860 by modified berlekamp–massey algorithm. *Computational and Applied Mathematics*,
861 43(2):102, 2024.
- 862 [8] Tariq Shah and Summera Said Rasool. On codes over quaternion integers. *Applicable*
863 *Algebra in Engineering, Communication and Computing*, 24(6):477–496, 2013.
- 864 [9] Mehmet Ozen and Murat Guzeltepe. Codes over quaternion integers. *European*
865 *Journal of Pure and Applied Mathematics*, 3(4):670–677, 2010.
- 866 [10] Mehmet Özen and Murat Güzeltepe. Cyclic codes over some finite quaternion integer
867 rings. *Journal of the Franklin Institute*, 348(7):1312–1317, 2011.
- 868 [11] Muhammad Sajjad, Tariq Shah, Mohammad Mazyad Hazzazi, Adel R Alharbi, and
869 Iqtadar Hussain. Quaternion integers based higher length cyclic codes and their
870 decoding algorithm. *Computers, Materials & Continua*, 73(1), 2022.
- 871 [12] Mohammad Mazyad Hazzazi, Muhammad Sajjad, Zaid Bassfar, Tariq Shah, and Ash-
872 wag Albakri. Nonlinear components of a block cipher over eisenstein integers. *Com-*
873 *puters, Materials & Continua*, 77(3), 2023.
- 874 [13] Muhammad Sajjad, Tariq Shah, and Robinson Julian Serna. Designing pair of non-
875 linear components of a block cipher over gaussian integers. *Computers, Materials &*
876 *Continua*, 75(3), 2023.
- 877 [14] Muhammad Sajjad, Tariq Shah, Huda Alsaud, and Maha Alammari. Designing pair of
878 nonlinear components of a block cipher over quaternion integers. *AIMS Mathematics*,
879 8(9):21089–21105, 2023.
- 880 [15] Firat Artuğer and Fatih Özkaynak. An effective method to improve nonlinearity value
881 of substitution boxes based on random selection. *Information Sciences*, 576:577–588,
882 2021.
- 883 [16] Ahmed A Abd EL-Latif, Bassem Abd-El-Atty, and Salvador E Venegas-Andraca.
884 Controlled alternate quantum walk-based pseudo-random number generator and its
885 application to quantum color image encryption. *Physica A: Statistical Mechanics and*
886 *its Applications*, 547:123869, 2020.
- 887 [17] Saleh Ibrahim and Ayman Alharbi. Efficient image encryption scheme using henon
888 map, dynamic s-boxes and elliptic curve cryptography. *IEEE Access*, 8:194289–
889 194302, 2020.
- 890 [18] Zeba Shamsi and Dolendro Singh Laiphrakpam. Securing encrypted image informa-
891 tion in audio data. *Multimedia Tools and Applications*, 82(21):33063–33085, 2023.
- 892 [19] Xingyuan Wang, Le Feng, and Hongyu Zhao. Fast image encryption algorithm based
893 on parallel computing system. *Information sciences*, 486:340–358, 2019.

- 894 [20] Guangfeng Cheng, Chunhua Wang, and Hua Chen. A novel color image encryption
895 algorithm based on hyperchaotic system and permutation-diffusion architecture.
896 *International Journal of Bifurcation and Chaos*, 29(09):1950115, 2019.
- 897 [21] Dania Saleem Malik and Tariq Shah. Color multiple image encryption scheme based
898 on 3d-chaotic maps. *Mathematics and Computers in Simulation*, 178:646–666, 2020.
- 899 [22] Qi Yin and Chunhua Wang. A new chaotic image encryption scheme using breadth-
900 first search and dynamic diffusion. *International Journal of Bifurcation and Chaos*,
901 28(04):1850047, 2018.
- 902 [23] Xing-Yuan Wang, Ying-Qian Zhang, and Xue-Mei Bao. A novel chaotic image en-
903 cryptation scheme using dna sequence operations. *Optics and Lasers in Engineering*,
904 73:53–61, 2015.
- 905 [24] SiCheng Wang, ChunHua Wang, and Cong Xu. An image encryption algorithm based
906 on a hidden attractor chaos system and the knuth–durstenfeld algorithm. *Optics and*
907 *Lasers in Engineering*, 128:105995, 2020.
- 908 [25] Minjun Zhou and Chunhua Wang. A novel image encryption scheme based on con-
909 servative hyperchaotic system and closed-loop diffusion between blocks. *Signal Pro-*
910 *cessing*, 171:107484, 2020.
- 911 [26] Xing-Yuan Wang and Zhi-Ming Li. A color image encryption algorithm based on
912 hopfield chaotic neural network. *Optics and Lasers in Engineering*, 115:107–118,
913 2019.
- 914 [27] Xingyuan Wang and Suo Gao. Image encryption algorithm for synchronously up-
915 dating boolean networks based on matrix semi-tensor product theory. *Information*
916 *sciences*, 507:16–36, 2020.
- 917 [28] Wei Liu, Zhenwei Xie, Zhengjun Liu, Yan Zhang, and Shutian Liu. Multiple-image
918 encryption based on optical asymmetric key cryptosystem. *Optics Communications*,
919 335:205–211, 2015.
- 920 [29] Y Xiong, C Quan, and CJ Tay. Multiple image encryption scheme based on pixel
921 exchange operation and vector decomposition. *Optics and Lasers in Engineering*,
922 101:113–121, 2018.
- 923 [30] Pingke Deng, Ming Diao, Mingguang Shan, Zhi Zhong, and Yabin Zhang. Multiple-
924 image encryption using spectral cropping and spatial multiplexing. *Optics Commu-*
925 *nications*, 359:234–239, 2016.
- 926 [31] Chun-Lai Li, Hong-Min Li, Fu-Dong Li, Du-Qu Wei, Xuan-Bing Yang, and Jing
927 Zhang. Multiple-image encryption by using robust chaotic map in wavelet transform
928 domain. *Optik*, 171:277–286, 2018.
- 929 [32] Xiaoqiang Zhang and Xuesong Wang. Multiple-image encryption algorithm based on
930 the 3d permutation model and chaotic system. *Symmetry*, 10(11):660, 2018.
- 931 [33] Xiaoqiang Zhang and Xuesong Wang. Multiple-image encryption algorithm based on
932 dna encoding and chaotic system. *Multimedia Tools and Applications*, 78(6):7841–
933 7869, 2019.
- 934 [34] Muhammad Sajjad, Tariq Shah, Rafik Hamza, Bander Almutairi, and Robinson Ju-
935 lian Serna. Multiple color images security by spn over the residue classes of gaussian
936 integer. *Scientific Reports*, 15(1):6425, 2025.

- 937 [35] Hongjun Liu, Jian Liu, and Chao Ma. Constructing dynamic strong s-box using 3d
938 chaotic map and application to image encryption. *Multimedia Tools and Applications*,
939 82(16):23899–23914, 2023.
- 940 [36] Lingfeng Qu, Fan Chen, Shanjun Zhang, and Hongjie He. Cryptanalysis of reversible
941 data hiding in encrypted images by block permutation and co-modulation. *IEEE*
942 *Transactions on Multimedia*, 24:2924–2937, 2021.